Structure, Volume *28*

Supplemental Information

Malleability of the SARS-CoV-2 3CL M^{pro} Active-Site Cavity Facilitates Binding of Clinical Antivirals

Daniel W. Kneller, Stephanie Galanie, Gwyndalyn Phillips, Hugh M. O'Neill, Leighton Coates, and Andrey Kovalevsky

Supplemental Information

Malleability of the SARS-CoV-2 3CL M^{pro} active site cavity facilitates binding of clinical antivirals

Daniel W. Kneller,[1,2] Stephanie Galanie,[2,3] Gwyndalyn Phillips,[1,2] Hugh M. O'Neill,[1,2] Leighton Coates,[2,4]* and Andrey Kovalevsky,[1,2]*ξ

[1]*Neutron Scattering Division, Oak Ridge National Laboratory, 1 Bethel Valley Road, Oak Ridge, TN, 37831, USA*

[2]*National Virtual Biotechnology Laboratory, US Department of Energy*

[3]*Biosciences Division, Oak Ridge National Laboratory, 1 Bethel Valley Road, Oak Ridge, TN, 37831, USA*

[4]*Second Target Station, Oak Ridge National Laboratory, 1 Bethel Valley Road, Oak Ridge, TN, 37831, USA*

[ξ]Lead contact

*Corresponding Authors: Leighton Coates: coatesl@ornl.gov, Andrey Kovalevsky: kovalevskyay@ornl.gov

Table S1. Data reduction and refinement statistics for the room temperature structures the 3CL M^{pro} from SARS-CoV-2 in complexes with inhibitors. Related to Figure 1.

	3CL M^{pro}-Leupeptin (293K) PDB ID 6XCH	**3CL M^{pro}-Telaprevir** (293K) PDB ID 6XQS	**3CL M^{pro}-Narlaprevir** (293K) PDB ID 6XQT	**3CL M^{pro}-Boceprevir** (293K) PDB ID 6XQU
Data collection:	**X-ray (in-house)**	**X-ray (in-house)**	**X-ray (in-house)**	**X-ray (in-house)**
Diffractometer	Rigaku HighFlux Eiger 4M	Rigaku HighFlux Eiger 4M	Rigaku HighFlux Eiger 4M	Rigaku HighFlux Eiger 4M
Space group	I2	C2	$P2_1$	I2
Wavelength (Å)	1.5406	1.5406	1.5406	1.5406
Cell dimensions:				
a, *b*, *c* (Å)	45.59, 53.35, 113.19	110.64, 55.60, 48.74	46.50, 54.48, 114.53	46.28, 53.46, 113.10
a, b, g (°)	90, 101.02, 90	90, 101.26, 90	90, 101.52, 90	90, 100.95, 90
Resolution (Å)	55.60-2.20 (2.28-2.20)*	55.24-1.90 (1.97-1.90)	112.2-2.30 (2.38-2.30)	55.57-2.20 (2.28-2.20)
No. reflections unique	13712 (1374)	22393 (1803)	25255 (2513)	13888 (1387)
R_{merge}	0.096 (0.503)	0.044 (0.308)	0.119 (0.752)	0.111 (0.654)
R_{pim}	0.061 (0.320)	0.026 (0.263)	0.066 (0.412)	0.062 (0.385)
$CC_{1/2}$	0.987 (0.696)	0.998 (0.838)	0.988 (0.518)	0.991 (0.441)
$I / \sigma I$	9.84 (1.86)	20.9 (2.29)	6.7 (0.72)	10.4 (1.21)
Completeness (%)	97.9 (97.6)	97.3 (78.3)	99.9 (99.4)	99.8 (99.7)
Redundancy	3.4 (3.3)	3.3 (1.8)	4.1 (4.1)	4.3 (3.9)
Refinement:				
R_{work} / R_{free}	0.1970/0.2370	0.1710.0.2039	0.2254/0.2769	0.1760/0.2338
Ramachandran statistics				
Favored (%)	96.05	97.37	94.08	96.05
Allowed (%)	3.95	2.63	5.92	3.95
Outliers (%)	0	0	0	0
R.M.S. deviations				
Bond lengths (Å)	0.003	0.012	0.006	0.008
Bond angles (°)	0.645	1.119	0.937	1.064
All atom clashscore	3.37	3.95	5.53	3.81

* Values in parentheses are for the highest-resolution shell.

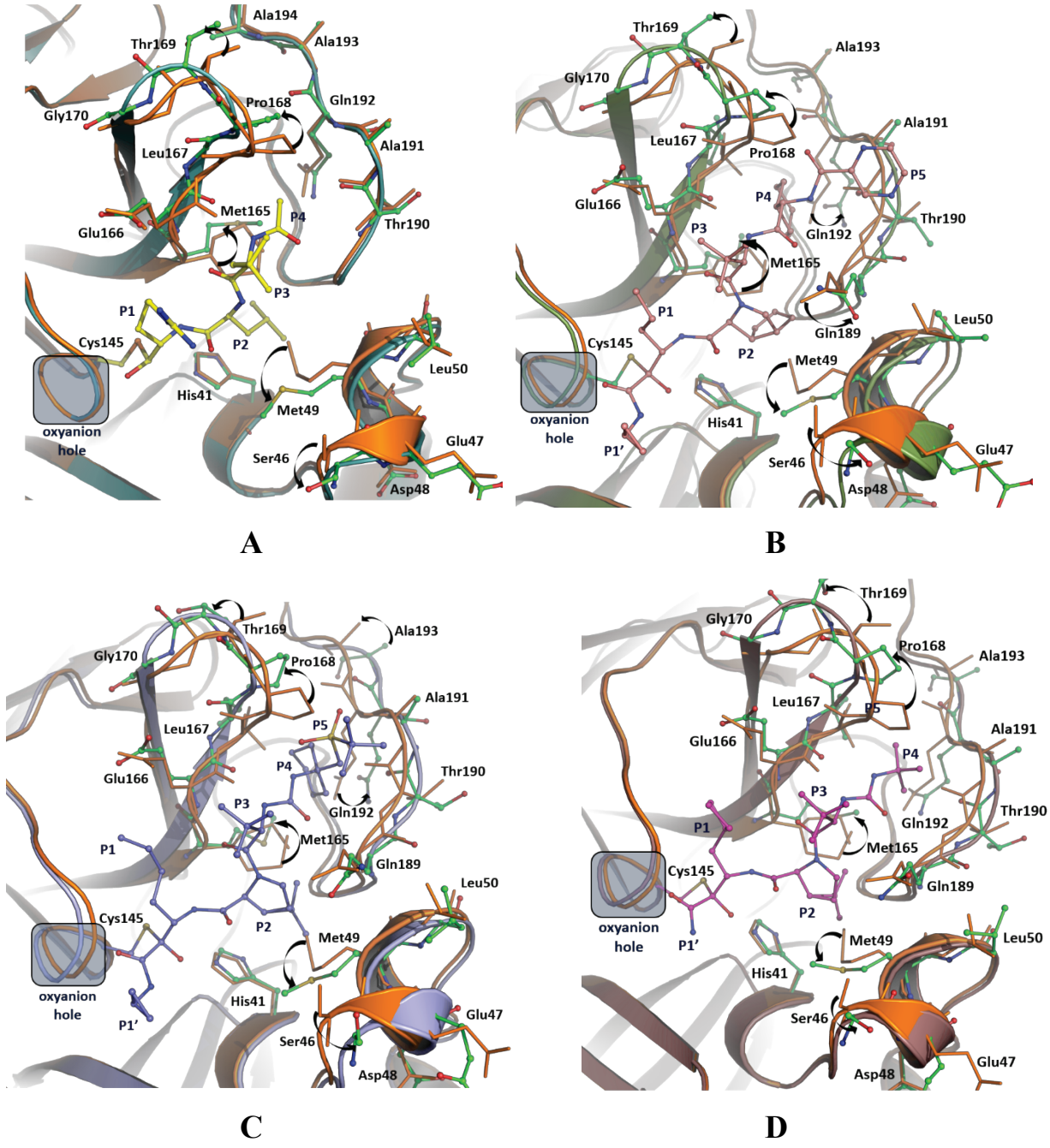

Figure S1. Conformational changes of the active site cavity caused by the inhibitor binding. (**A**) 3CL M^{pro}-leupeptin complex is shown in ball-and-stick representation (yellow and green carbons) and dark teal cartoon. (**B**) 3CL M^{pro}-telaprevir complex is shown in ball-and-stick representation (dark pink and green carbons) and smudge cartoon. (**C**) 3CL M^{pro}-narlaprevir complex. (**D**) 3CL M^{pro}-boceprevir complex. Ligand-free enzyme (PDB ID 6WQF) is shown in stick representation and is colored orange in all panels. Related to Figure 4.

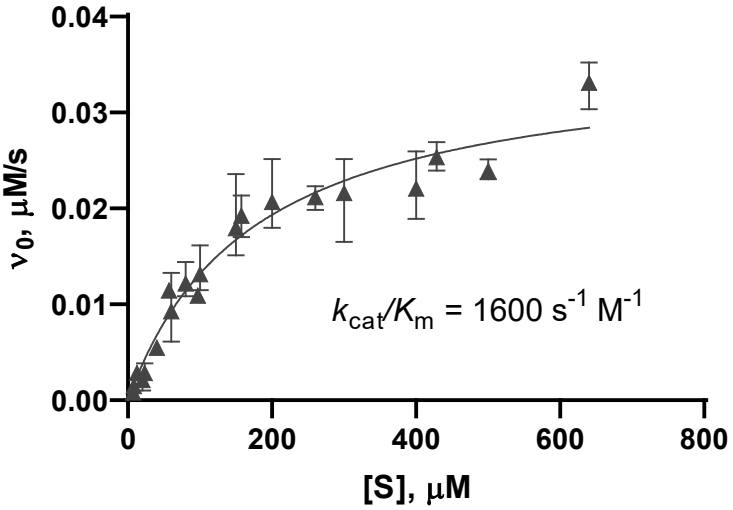

Figure S2. SARS-CoV-2 main protease kinetic characterization. Points represent the average of n = 3 initial rates of FRET peptide substrate cleavage by 130 nM enzyme over a range of substrate concentrations. Error bars represent the standard deviations of these triplicates, and two independent experiments are plotted with slightly different substrate concentrations. The line indicates the nonlinear regression of the Michaelis-Menten equation to the data with GraphPad Prism v. 8.4.2. The best-fit parameters were V_{max} = 36 nM/s EDANS released/second 95% CI [32, 41], giving k_{cat} = 0.28 s^{-1}, and K_M = 170 µM peptide substrate 95% CI [130, 230]. Related to STAR Methods.

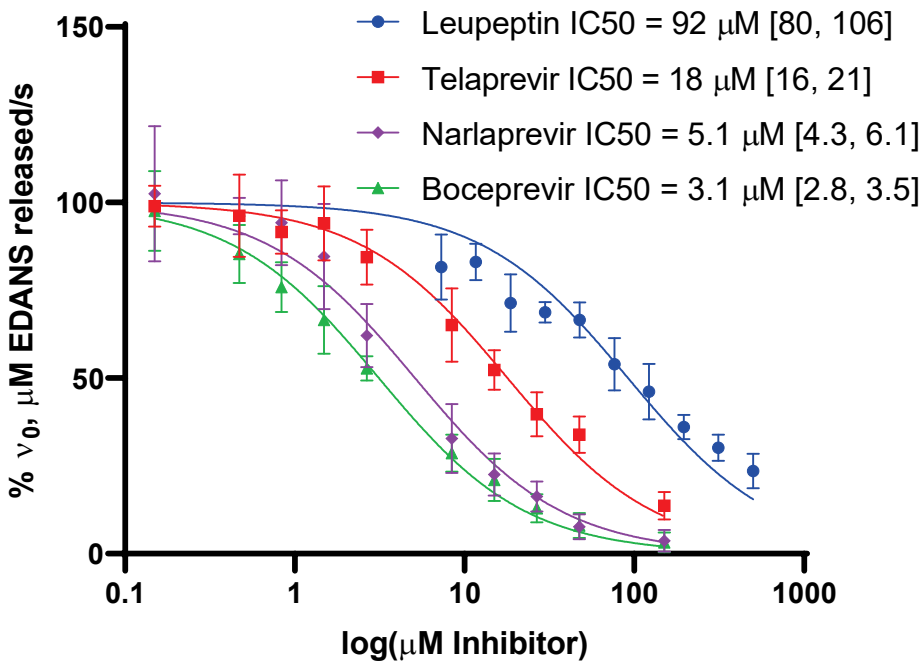

Figure S3. *In vitro* biochemical inhibition of main protease. Initial rates across the concentration range are normalized to no inhibitor control (100% activity) and no enzyme control (0% activity). Error bars are standard deviation of two independent experiments, each performed in triplicate. Lines indicate the nonlinear regression of the [Inhibitor] vs. normalized response IC50 equation to the data with GraphPad Prism. Bracketed values in the legend represent 95% confidence intervals for IC50 from the regression. Related to STAR Methods.

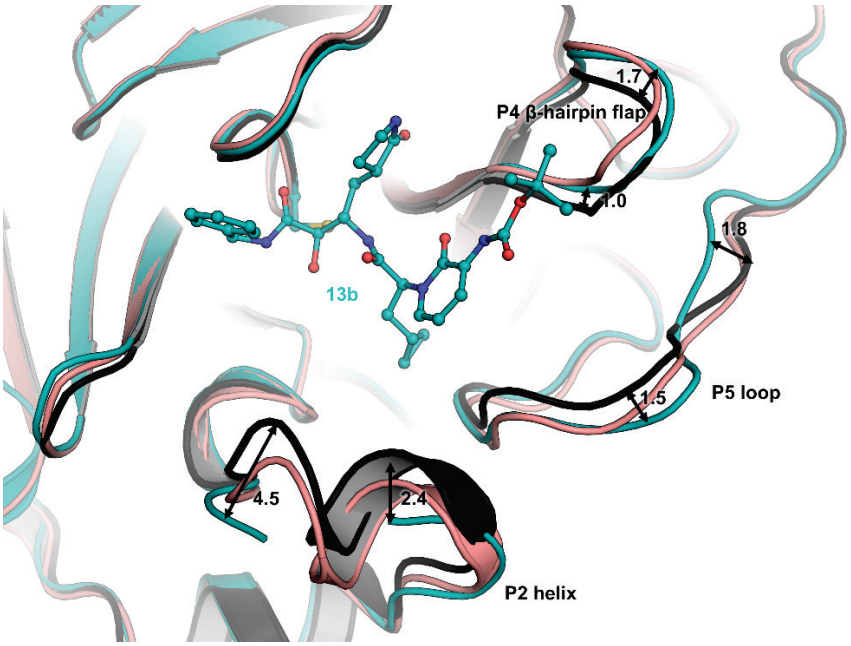

A

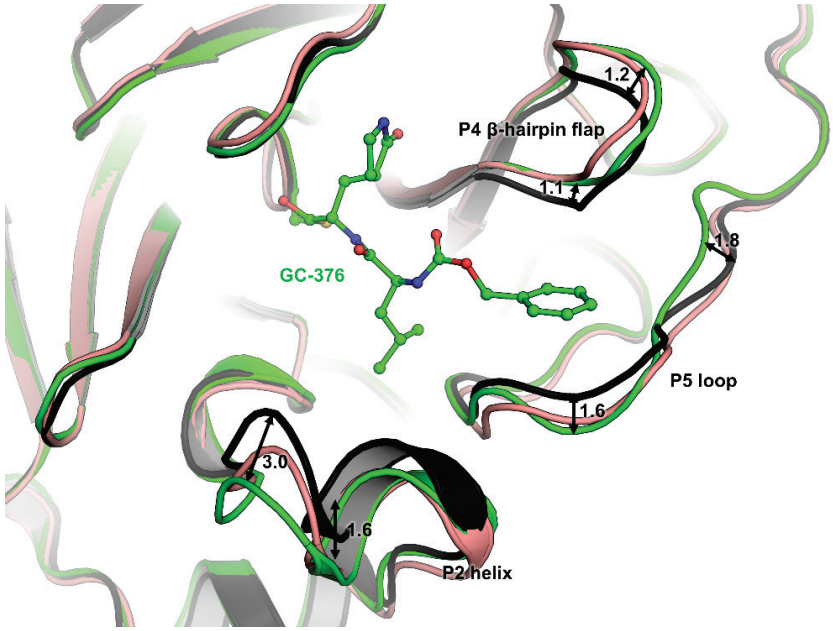

B

Figure S4. Comparison of the conformational changes of the active site cavity in SARS-CoV-2 3CL M^{pro} caused by inhibitor binding. (**A**) Ligand-free 3CL M^{pro} (PDB ID 6WQF) shown is black is superimposed with 3CL M^{pro}-13b (PDB ID 6Y2F) and 3CL M^{pro}-telaprevir complexes shown in cyan and dark pink, respectively. The ketoamide inhibitor 13b is shown in ball-and-stick representation. (**B**) Ligand-free 3CL M^{pro} (PDB ID 6WQF) shown is black is superimposed with 3CL M^{pro}-GC-376 (PDB ID 6WTT) and 3CL M^{pro}-telaprevir complexes shown in green and dark pink, respectively. The aldehyde inhibitor GC-376 is shown in ball-and-stick representation. Related to Figure 4.